

Article

Visual Comfort Analysis of Semi-Transparent Perovskite Based Building Integrated Photovoltaic Window for Hot Desert Climate (Riyadh, Saudi Arabia)

Aritra Ghosh ^{1,*} , Abdelhakim Mesloub ² , Mabrouk Touahmia ² and Meriem Ajmi ³ ¹ College of Engineering, Mathematics and Physical Sciences, Renewable Energy, University of Exeter, Cornwall TR10 9FE, UK² Department of Architectural Engineering, Ha'il University, Ha'il 2440, Saudi Arabia; a.maslub@uoh.edu.sa (A.M.); m.touahmia@uoh.edu.sa (M.T.)³ Research Laboratory of Metrology and Energy Systems, LR18ES21, National Engineering School, University of Monastir, Monastir 5060, Tunisia; ajm.meriem@gmail.com

* Correspondence: a.ghosh@exeter.ac.uk

Abstract: Buildings consume considerable amount of energy to maintain comfortable interior. By allowing daylight, visual comfort inside a building is possible which can enhance the occupant's health, mood and cognitive performance. However, traditional highly transparent windows should be replaced with semitransparent type window to attain a comfortable daylight inside a building. Evaluation of visual comfort includes both daylight glare and colour comfort analysis. Building integrated photovoltaic (BIPV) type windows are promising systems and can possess a range of semitransparent levels depending on the type of PV used. In this work, the semitransparent Perovskite BIPV windows was investigated by employing daylight glare analysis for an office building located in Riyadh, KSA and three wavelength dependent transmission spectra for colour comfort analysis. The results showed that the transmissions range between 50–70% was optimum for the comfortable daylight for south facing vertical pane BPV-windows. However, excellent colour comfort was attained for the transmission range of 90% which provided glare issues. Colour comfort for 20% transparent Perovskite was compared with contemporary other type of PV which clearly indicated that wavelength dependent transmittance is stronger over single value transmittance.

Keywords: BIPV; window; perovskite; CCT; CRI; glare; visual comfort; Saudi Arabia



Citation: Ghosh, A.; Mesloub, A.; Touahmia, M.; Ajmi, M. Visual Comfort Analysis of Semi-Transparent Perovskite Based Building Integrated Photovoltaic Window for Hot Desert Climate (Riyadh, Saudi Arabia). *Energies* **2021**, *14*, 1043. <https://doi.org/10.3390/en14041043>

Academic Editor: Gregorio García

Received: 10 January 2021

Accepted: 14 February 2021

Published: 17 February 2021

Publisher's Note: MDPI stays neutral with regard to jurisdictional claims in published maps and institutional affiliations.



Copyright: © 2021 by the authors. Licensee MDPI, Basel, Switzerland. This article is an open access article distributed under the terms and conditions of the Creative Commons Attribution (CC BY) license (<https://creativecommons.org/licenses/by/4.0/>).

1. Introduction

Currently, the Buildings sector consumes about 40% of the global energy to maintain buildings' interior comfort for occupants. In 2019, total energy consumption for building sector reached 128EJ which was 7% higher than in 2010. Because of this high consumption, CO₂ emission from building sector increased by 5% compared to 2010 level [1]. To achieve the building interior comfort, energy consumption and greenhouse gas emission due to the buildings sector have increased tremendously over the last decade, and have even exceeded the transport sector consumption [2,3]. To meet the united nation climate change target, energy demand reduction from buildings consumption is essential. Reducing artificial lighting energy demand by allowing suitable daylight penetration is one of the best approaches. Building occupants mostly spend over 90% of their time inside the building. Thus to improve the cognitive performance of building occupants, interaction between external world and building interior is essential by allowing daylight [4,5]. Daylight enhances the health, awareness, productivity, and sense of comfort play crucial role for building indoor. Suitable daylight improves the visual comfort while excessive amount creates discomfort. Understanding the quality and quantity of daylight in buildings is thus crucial to satisfy the indoor occupant comfort [6]. Daylighting glare, correlated colour

temperature (CCT) and colour rendering index (CRI) are the three crucial components to understand the visual comfort [7–9].

Buildings include different components such as windows, walls, roofs, and doors. Windows are the only transparent part of a building which allow external daylight to building interior. Presently, single and double glass pane based windows are commercially popular [10]. However, they are not suitable for comfortable daylight because of their high transparency. Poor daylight distribution and excessive illumination can create visual comfort issues. Currently, building window systems are divided based on their transmission property. Switchable and non-switchable are the two available types of window systems. Switchable windows are smart window type which have more than one transparency and can be modulated based on electrical and thermal impulse [11–16]. Non switchable advanced windows are primarily for cold climate dominated aerogel and vacuum glazing and hot climate dominated PV window [17]. PV windows can also be known as building integrated photovoltaic (BIPV) windows as they replaced the traditional building envelopes [18–20]. BIPV windows have triple point advantages as they generate onsite power, control admitted solar heat and light, and aesthetic [21]. Energy renovation with BIPV is promising for urban building context [22]. For daylight and building aesthetic application BIPV windows need to be semi-transparent. PV system for BIPV windows can be first, second or third generation type of PV. The first generation silicon is the most mature technology but is opaque in nature and has efficiency limit [23,24]. The second and third generation PV systems are suitable for BIPV windows application because of the tuneable transparency nature of the PV cells. The second generation a-Si [25], CdTe [26,27] and CIGS have been employed before to investigate as BIPV window. The third generation organic [28], DSSC [29] and Perovskite [30] are also now taking high importance in PV application because of their simple fabrication. In the last several years, Perovskite PV showed tremendous improvements and their efficiency closely matched to inorganic type PV cells [31]. Moreover, temperature coefficient of Perovskite technology has weaker temperature impact compared to first and second generation PV systems [32]. Perovskite PVs still suffer from long term stability and use of lead has environmental concern. However, they are still under consideration because of the enormous improvement in their efficiency (from ~3% to ~22) within 10 years compared to silicon solar cell which took three decades to reach this amount of improvement [33].

In terms of toxicity, the employed lead in PSCs is not very significant and comparatively this amount is much less than the amount of lead used in lead-cadmium batteries. Moreover, the amount of employed lead in soldering of commercial Si PV systems are much higher than the lead being used in Perovskite PV (only 0.4 g/m²) [34]. Use of BIPV window system over clear window creates coloured appearance [35]. Though c-Si cells look like typical blue colour because of the antireflecting coating, Si based window is built by maintaining spacing between cells [36]. Thus, entering daylight remains similar to external daylight and spectrum distortion chance is limited or rare [37]. For 2nd generation thin film, it's also similar to c-Si types. For third generation, the colour of the cells looks different because of the employment of different coloured dyes and components [38]. Entering light through the BIPV system can have different spectrum than the external daylight. Distorted entering external daylight spectrum inside a building interior can create issues.

Attaining visual comfort is critical for hot climate. Building energy consumption is very high in hot and humid regions such as Kingdom of Saudi Arabia (KSA), which experiences harsh desert climate throughout the year and receives close to 2000 kWh/m² solar exposure yearly [39]. Buildings at KSA are exposed to this considerable amount of solar radiation and harsh climate. Thus, to maintain indoor comfort, the KSA has the highest share of electricity consumption, being responsible for consuming 76% of the total energy of which 70% of energy is only consumed to satisfy cooling load demand [40]. The residential building sector in KSA is responsible for almost 50% of the total national electricity consumption which is expected to be double in the next 5 years. The root cause of this problem is the subsidized electricity tariffs, high growth rate of population and building,

use of outdated building construction material, and lack of policies/- codes/incentives to develop energy efficient buildings. As this oil-driven electricity generation has an adverse impact on the environment, the KSA has set the target to abate the carbon emission up to 130 million tons by 2030 [41]. Abatement of building energy consumption is thus utmost important to reach this goal. Current building window systems in the KSA are double pane type which does not meet the standard set by the Saudi government. Because of the high transmission window, shading devices are often employed to eliminate the excessive entering daylight. Visual comfort and energy consumption using light shelves in Saudi climate was previously investigated. It was found that light shelves having height of 1.3 m, the addition of a 30 cm reflector on the top of a window can abate over 85% of the energy consumption and eliminates uncomfortable glare [42]. Another study evaluated the energy saving and visual comfort of 20% transparent second generation PV which saved 58% of building energy by [43]. It is also claimed that 12.25 kW PV system is required for a typical Saudi Arabian apartment [44]. Investigations of PV technology in other hot climate regions such as Dubai [45] and Kuwait [46] were also performed.

The literature review showed that only few studies related to PV integrated to buildings, particularly BIPV windows and visual comfort for BIPV window systems, have been conducted in KSA. In this work, semi-transparent Perovskite PV based BIPV windows for Saudi climate is investigated by employing daylight glare and colour comfort analysis. For comparison, other generations of PVs are also employed. How visual comfort analysis get affected because of single value transmittance and wavelength dependent transmission has been evaluated and discussed broadly.

2. Materials and Methods

This theoretical study was performed considering the climatic data of Riyadh (24.694973° N, 46.724133° E) city capital of Saudi Arabia and the largest city on the Arabian Peninsula. Under Kopean climate classification, it is a hot desert climate having above 45 °C ambient temperature in the summer and below 5 °C in the winter. The area receives intense solar radiation over the course of the year as shown in Figure 1. The monthly maximum global horizontal radiation varies from 236 kWh/m² in summer to 131 kWh/m² in winter. This area experiences over 60% clear skies in an average year, while 40% of the days are overcast or mostly cloudy. Presence of daylight varies from 10.6 to 13.6 h which is a clear indication of daylight availability throughout the year for this location.

To adequately assess the visual comfort characteristics of the current semi-transparent Perovskite based BIPV windows, a series of simulations were performed for a small office prototype which characterizes common offices in Riyadh City. This prototype was designed with a curtain wall and fixed window-to-wall ratio (WWR) of 100% (fully glazing). The geometric dimension is 3.00 × 4.00 m² and 3.0 m in height, lateral in typology, and has south-facing office units with no shading from adjacent buildings as presented in Figure 2. The typical meteorological year of Riyadh city was used Meteoronorm data-base; in particular the average of external illuminance levels, to determine the visual discomfort glare inside the prototype office.

For the radiance simulation, Diva-for-Rhino program was employed, and the given input parameters are listed in Tables 1 and 2. For this type of analysis, a knowledge of materials reflection values are very important to ensure the photometric accuracy.

For the Semi-transparent perovskite BIPV window, transmission was varied from 10 to 90% which are single-value visual transmittance. In addition, wavelength dependent three different Perovskite was selected for this study to analysis the colour comfort work shown in Figure 3. For comparison with other types of PV, DSSC and CdTe are selected as shown in Figure 4. Average visual transmission was calculated using Equation (1).

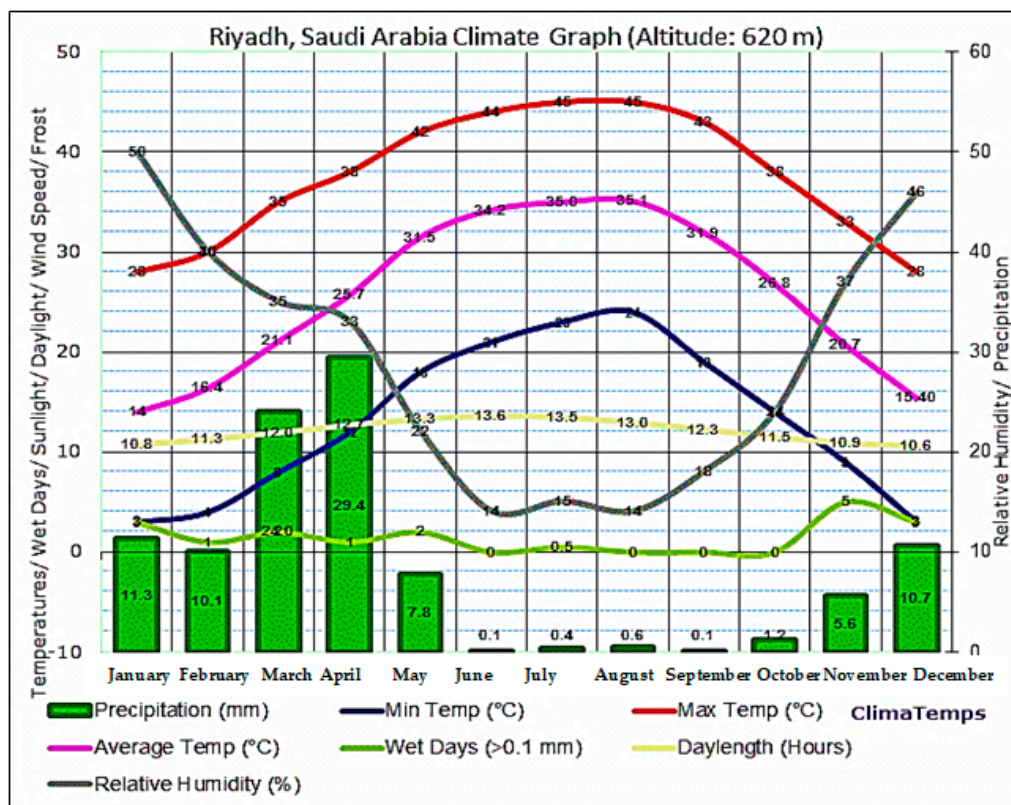


Figure 1. Climatic data of Riyadh city based on Kopean climate classification.

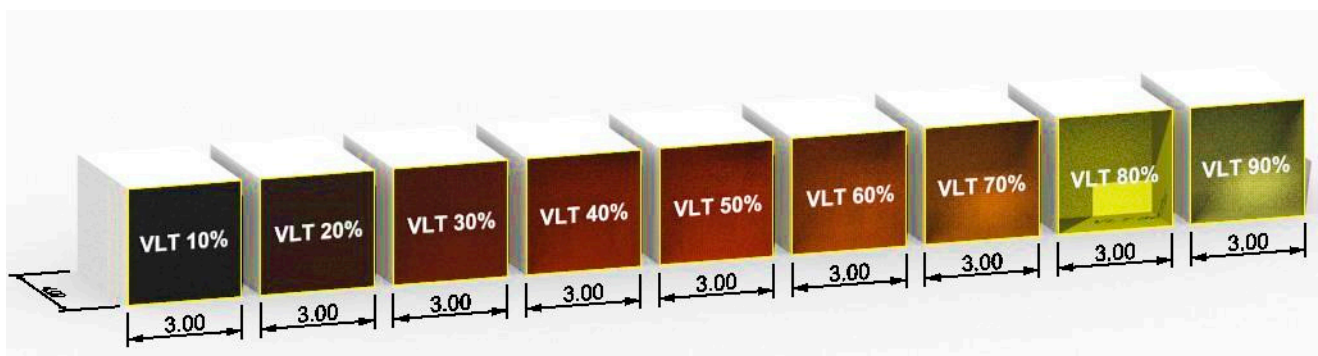


Figure 2. Schematic of geometric dimension of south facing prototype office building in Riyadh, window to wall ratio 1:1. Window transmission changed from 10% to 90%.

Table 1. Material reflection coefficient percentage.

Material	Reflection Coefficient (%)
Generic Ceiling	70
Generic Floor	20
Generic Wall	50
Glazing (VLT)	From 10% to 90%

Table 2. Radiance parameters used in daylighting simulation.

Radiance Parameters	Value
Ambient bounces	7
Ambient divisions	1500
Ambient sampling	100
Ambient accuracy	0.05
Ambient resolution	300

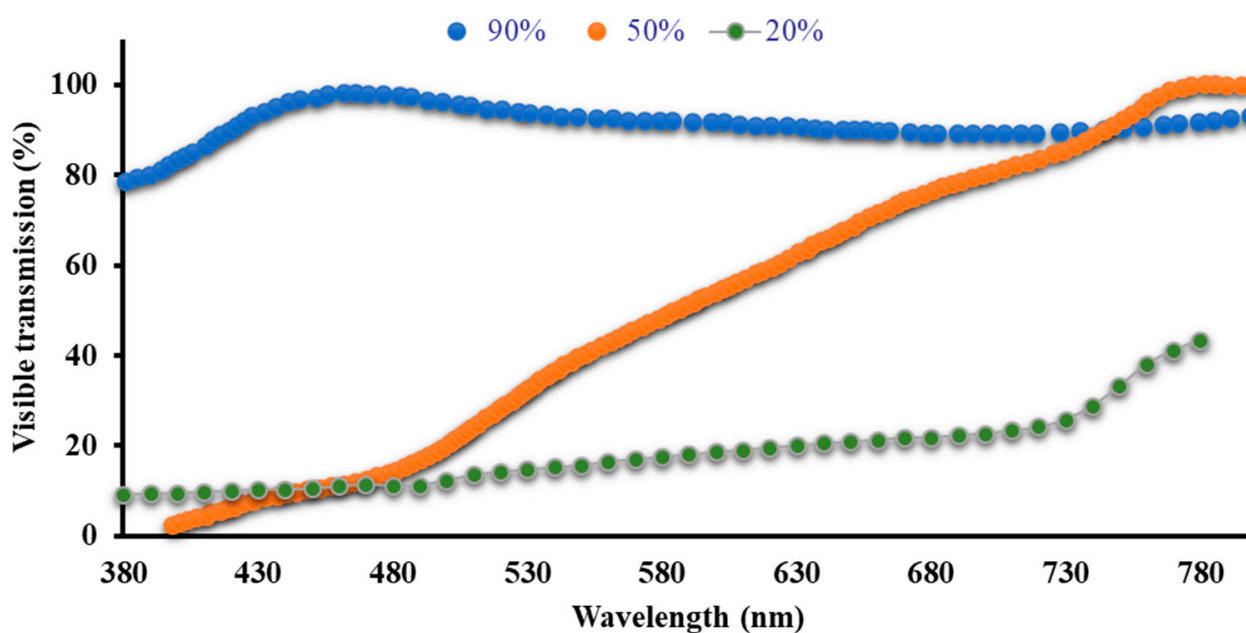


Figure 3. Wavelength dependent visible transmission for 20% [47], 50% [48] and 90% [49] semi-transparent Perovskite cell for BIPV window. 20%, 50% and 90% Graphs are reproduced from [47–49] respectively. Reprint with permission [47], 2021, Elsevier and [48,49]; 2021, John Wiley and Sons.

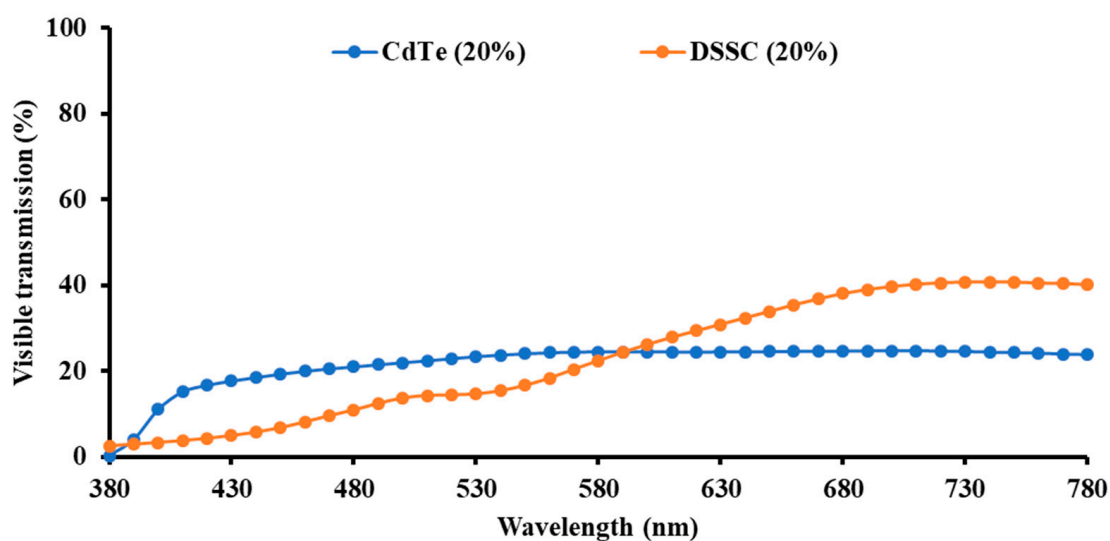


Figure 4. Wavelength dependent visible transmission for 20% CdTe [50], DSSC 20% [51]. Graphs are reproduced from [50,51]. Reprint with permission [50,51], 2021, Elsevier.

Average visible light transmittance values τ_v are given by [52]:

$$\tau_v = \frac{\sum_{380\text{nm}}^{780\text{nm}} D_{65}(\lambda) V(\lambda) \tau(\lambda) \Delta\lambda}{\sum_{380\text{nm}}^{780\text{nm}} D_{65}(\lambda) V(\lambda) \Delta\lambda} \quad (1)$$

where $\tau(\lambda)$ is the wavelength dependent transmission of BIPV window, $D_{65}(\lambda)$ represents the spectral power distribution of CIE standard illuminant, D_{65} , $V(\lambda)$ indicate the photopic luminous efficiency function of the human eye and $\Delta\lambda = 10 \text{ nm}$.

Visual Comfort Analysis

To understand and evaluate visual comfort, knowledge of both quality and quantity indoor daylight is indispensable. Daylight glare is the indicator of quality of daylight while quantity is evaluated by CRI and CCT [53]. In this study, the analysis was conducted using the daylight glare probability (DGP) measure in order to identify discomfort glare. A rendering 3D map contour image that could replace the HDR image in the direction looking at the semi-transparent BIPV window at 1.12 m (eye-level height of a person sitting on a chair at each point) was performed at solstice winter (21 December 2020 and summer (21 June 2020) which is considered a critical period; in 9.00 a.m., 12.00 p.m., 3.00 p.m. under clear sky condition (common sky condition in Riyadh city).

The performance indicator of visual comfort was employed in this study and presented in Table 3. Discomfort glare is created by the direct sunlight and from bright skylight and it is a direct function of both the size of the window and the brightness of the sky seen through it. Glare can therefore be reduced by cutting down the size of window or reducing the transmissivity of the window. Discomfort glare is a sensation of pain caused by luminance which is higher than the limit of eyes adaptation. Working under discomfort glare ambience may not create any direct disturbance on the occupants working performance but create physiological symptoms such as headache. This will affect the production and performance of the work indirectly. Simplified daylight glare probability (DGP) as shown in Equation (2) was developed to evaluate glare by using just vertical illuminance (E_v) which can be measured or calculated. Required DGP is listed in Table 3.

$$DGP = 6.22 \times 10^{-5} E_v + 0.184 \quad (2)$$

Table 3. The performance indicator of daylight glare probability (DGP).

Criteria	Performance Indicator of Daylighting Quality
DGP	0.35 < imperceptible glare
	0.35–0.40 perceptible glare
	0.4–0.45 disturbing glare
	>0.45 intolerable glare

CCT and CRI evaluate the colour comfort that is essential to understand the visual comfort fully. CCT of transmitted daylight through window should remain between 3000 K and 7500 K. The CCT of an overcast sky is 6000 K while 10,000 K for light blue sky [54]. CRI values over 80 are good while over 90 are considered to be excellent [6,7]. Good CCT and CRI indicate no significant colour difference between external daylight and the transmitted daylight through the window [55]. Lower the difference better the quality of light in to an indoor space which is an essential criteria for occupant's health, interpersonal relationships and aesthetic taste [56,57].

CRI and CCT are given by the following Equations (3) and (4) [58,59]:

$$CRI = \frac{1}{8} \sum_{i=1}^8 \left[100 - 46 \left\{ \sqrt{(U_{t,i}^* - U_{r,i}^*)^2 + (V_{t,i}^* - V_{r,i}^*)^2 + (W_{t,i}^* - W_{r,i}^*)^2} \right\} \right] \quad (3)$$

where W^* , U^* , V^* are the transform of the chromatic adaptation of the reference and test illuminant for the reflected light from each of the eight sample tests [60].

Colour space system $W_{t,i}^*$, $U_{t,i}^*$, $V_{t,i}^*$ are given by

$$\begin{aligned} W_{t,i}^* &= 25 \left(\frac{100Y_{t,i}}{Y_t} \right)^{1/3} - 17 \\ U_{t,i}^* &= 13W_{t,i}^* (u'_{t,i} - 0.1978) \\ V_{t,i}^* &= 13W_{t,i}^* (v'_{t,i} - 0.3122) \\ CCT &= 449n^3 + 3525n^2 + 6823.3n + 5520.33 \end{aligned} \quad (4)$$

3. Results

Table 4 shows the discomfort glare caused by the different transmission level of semi-transparent perovskite based BIPV window for 21 December 2020. 3D illuminance contour map and daylight glare probability (DGP) both were employed to evaluate the glare control potential. For 21 December 2020 at 9 am, maximum DGP was 50 and minimum was 7.3 for transmission level 90% and 10%. At 12pm, DGP increased from 9am and for the transmission.

An imperceptible glare for all three hours was achieved while transmission was 70% for this particular location and office. The maximum contour illuminance map within tested office increased from 10klux with 10% transmission to 40klux with 90% due to when the low sun position and its direct view. At 80% and 90% transmission, Perovskite BIPV window was not able to control the discomfort glare, where disturbing and intolerable glare clearly appeared leading to visual discomfort.

Table 5 shows the discomfort glare caused by the different transmission level of semi-transparent perovskite based BIPV window for 21 June 2020. The most critical part to control the glare is during mid-day period (12 PM) with high transmission, which is perceptible glare with 70% transmission to intolerable glare with 90%. While the DGP state at morning and evening periods is within visual comfort range. The highest contour illuminance map is much less than winter season which does not exceed 12klux with high transmission level.

CRI and CCT were calculated using Equation (3) and (4), respectively. Figure 5 shows the CCT and CRI for three wavelength dependent transmission of semi-transparent BIPV window (as mentioned in the methodology section). Interestingly, it is observed that 20% average visible transmission window possess higher CRI than 50% transparent window. It is noteworthy that CRI does not depend on single value transmittent but depends on the full wavelength dependent transmission in the visible wavelength. For 20% transparent Perovskite BIPV window, CCT and CRI are 4457 K and 80.52 while 50% transparent BIPV window, CRI and CCT are 56.72 and 3144 K. For 90% transparent window, 97.78 and 6815 are the CRI and CCT respectively. In terms of CCT and CRI, 90% transparent shows the best performance however in the previous section it was observed that it offered highest discomfort. Hence, combined the 50% transparent shows intermediate glare control compared to 20% and 90% transparent window but its colour comfort performance is poor. 90% transparent BIPV window is similar to single glazing which is not potential to control the visual comfort. Figure 6 represents the CCT and CRI between 20% transparent Perovskite, CdTe and DSSC based BIPV window. CRI is maximum for CdTe, which was >90 and Perovskite is 80 while DSSC is 59. Two crucial facts are established here that single value transmittance is not an adequate parameter to understand the colour comfort. In addition, an interesting fact is that daylight glare was evaluated with single value transmission. However, in the visible transmission equation, it was weighted corrected values, but the final single value does not make any difference between the different types of PV cells but has influential variation in the colour comfort analysis.

Table 4. The Daylight glare probability analysis with illuminance contour map at winter solstice 21 December 2020 (9am, 12pm and 3pm).










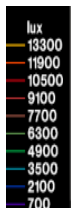
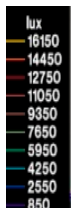
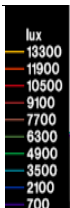

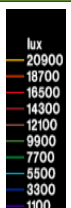
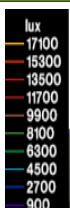
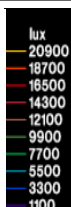
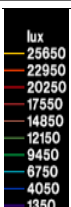
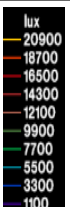
	9.00AM	12.00PM	3.00PM
VLT 10%			
	DGP = 0.07	DGP = 0.01	DGP = 0.08
VLT 20%			
	DGP = 0.12	DGP = 0.15	DGP = 0.13
VLT 30%			
	DGP = 0.18	DGP = 0.19	DGP = 0.19
VLT 40%			
	DGP = 0.21	DGP = 0.22	DGP = 0.219
VLT 50%			
	DGP = 0.25	DGP = 0.27	DGP = 0.25
VLT 60%			
	DGP = 0.29	DGP = 0.32	DGP = 0.30

Table 4. Cont.

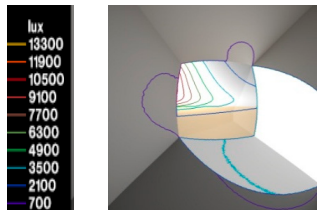
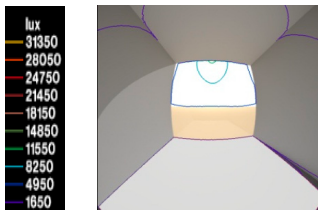
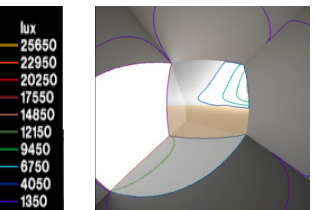
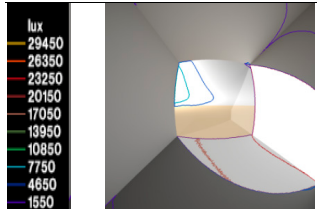
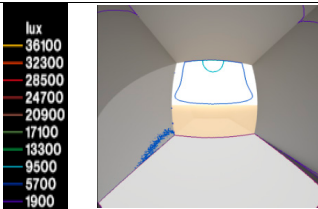
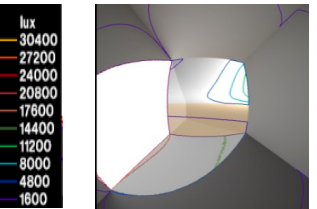
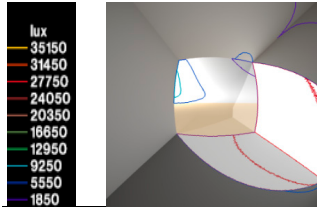
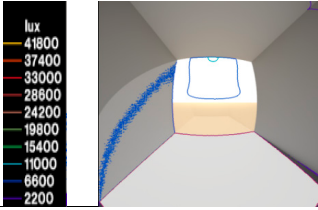
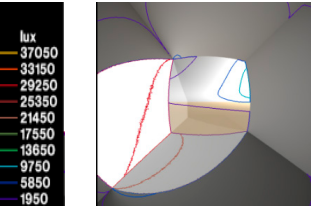
	9.00AM	12.00PM	3.00PM
VLT 70%	 DGP = 0.35	 DGP = 0.39	 DGP = 0.37
VLT 80%	 DGP = 0.418	 DGP = 0.469	 DGP = 0.44
VLT 90%	 DGP = 0.50	 DGP = 0.56	 DGP = 0.53

Table 5. The Daylight glare probability analysis with illuminance contour map at summer solstice 21 June 2020 (9am, 12pm, and 3pm).

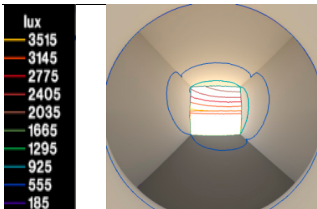
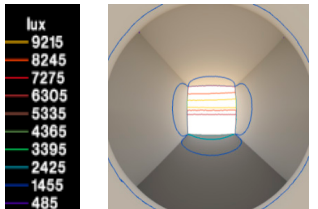
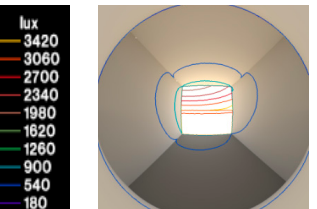
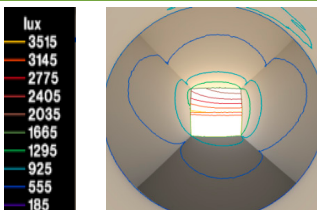
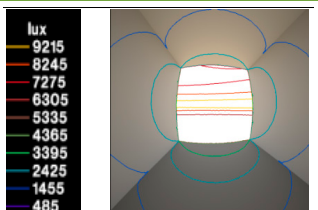
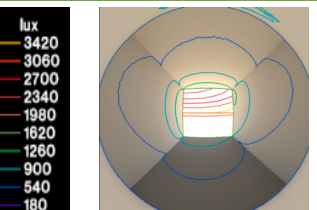
	9.00AM	12.00PM	3.00PM
VLT 60%	 DGP = 0.24	 DGP = 0.29	 DGP = 0.23
VLT 70%	 DGP = 0.26	 DGP = 0.38	 DGP = 0.25

Table 5. Cont.

	9.00AM	12.00PM	3.00PM
VLT 80%			
	DGP = 0.27	DGP = 0.46	DGP = 0.27
VLT 90%			
	DGP = 0.32	DGP = 0.55	DGP = 0.31

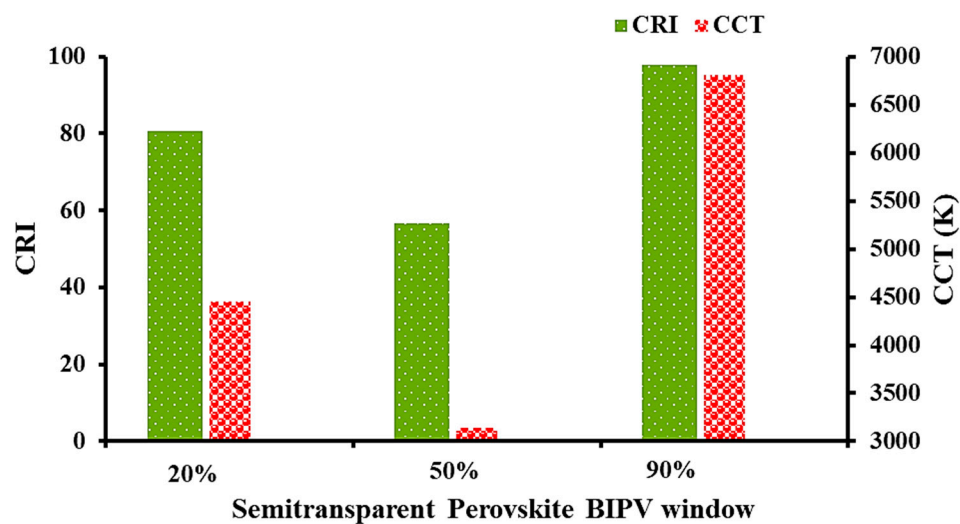


Figure 5. CCT and CRI analysis to evaluate colour comfort using three different transparent Perovskite based BIPV window.

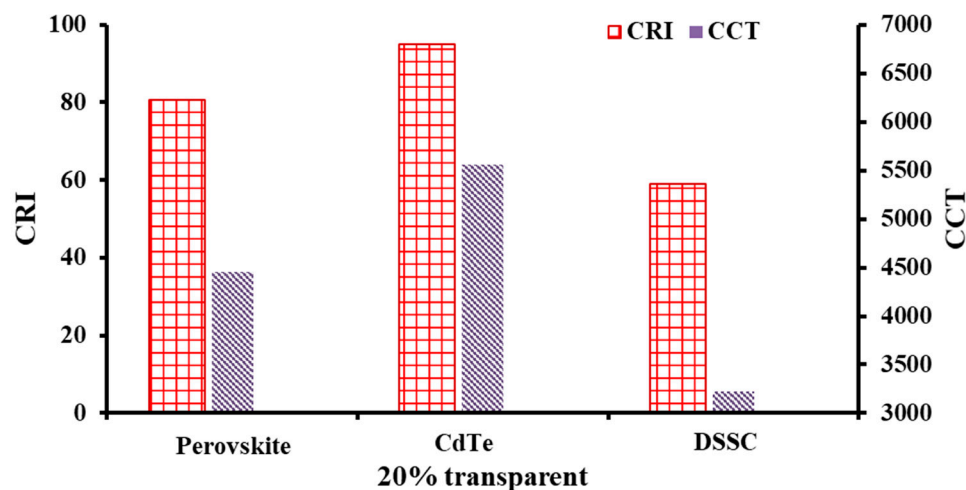


Figure 6. CCT and CRI analysis to evaluate colour comfort using three different type (Perovskite, CdTe, and DSSC) 20% transparent BIPV window.

4. Discussion and Conclusions

In this work, average visible light transmission was varied from 10% to 90% for Perovskite PV based BIPV window to evaluate the visual comfort for an office building in Riyadh, KSA. Two particular days (21 December 2020 and 21 July 2020) were selected for daylight glare control probability, as those days were representing winter and summer conditions. It was found that for wintertime the average visual transmission is below 50% and above 70% which is not suitable for visual comfort. For summer condition, 70% was promising but mid-day period was always crucial to control glare. Three-wavelength dependent transmission for three different BIPV window was also employed for colour comfort analysis, which is also a key part to understand visual comfort. 90% transparent window was found to have the excellent CCT and CRI, however based on the DGP it was not suitable. On the other hand, 20% transparent window which has imperceptible DGP showed allowable CCT and CRI. Compared CCT and CRI between DSSC and CdTe type with Perovskite clearly showed that wavelength dependent transmission values are significant over single value transmittance. Thus, it is recommended that to better understand visual comfort both analyses are crucial before making any final decision with semi-transparent perovskite and other types of PV based BIPV windows for building integration.

Author Contributions: Conceptualization, A.G.; methodology, A.G., A.M.; software, A.G., A.M.; validation, A.G., A.M.; formal analysis, A.G., A.M.; investigation, A.G.; resources, A.G., A.M.; data curation, A.G., A.M.; writing—original draft preparation, A.G., A.M.; writing—review and editing, A.G., A.M.; visualization, A.G., A.M.; supervision, A.G., A.M., M.T. and M.A.; project administration, A.G., A.M., M.T. and M.A.; funding acquisition, A.M., M.T. and M.A. All authors have read and agreed to the published version of the manuscript.

Funding: This research was funded by Research Deanship in University of Ha'il, Saudi Arabia grant number [RG-20 105].

Institutional Review Board Statement: Not applicable.

Informed Consent Statement: Not applicable.

Acknowledgments: This research has been funded from Research Deanship in University of Ha'il, Saudi Arabia, through Project no. RG-20 105.

Conflicts of Interest: The authors declare no conflict of interest.

References

1. IEA Tracking Building. 2020. Available online: <https://www.iea.org/reports/tracking-buildings-2020> (accessed on 30 December 2020).
2. Bhattacharjee, A.; Mohanty, R.K.; Ghosh, A. Design of an Optimized Thermal Management System for Li-Ion Batteries under Different Discharging Conditions. *Energies* **2020**, *13*, 5695. [\[CrossRef\]](#)
3. Ghosh, A. Possibilities and Challenges for the Inclusion of the Electric Vehicle (EV) to Reduce the Carbon Footprint in the Transport Sector: A Review. *Energies* **2020**, *13*, 2602. [\[CrossRef\]](#)
4. Ghosh, A.; Norton, B.; Duffy, A. Daylighting performance and glare calculation of a suspended particle device switchable glazing. *Sol. Energy* **2016**, *132*, 114–128. [\[CrossRef\]](#)
5. Ghosh, A.; Norton, B.; Mallick, T.K. Daylight characteristics of a polymer dispersed liquid crystal switchable glazing. *Sol. Energy Mater. Sol. Cells* **2018**, *174*, 572–576. [\[CrossRef\]](#)
6. Shafavi, N.S.; Zomorodian, Z.S.; Tahsildoost, M.; Javadi, M. Occupants visual comfort assessments: A review of field studies and lab experiments. *Sol. Energy* **2020**, *208*, 249–274. [\[CrossRef\]](#)
7. Andargie, M.S.; Touchie, M.; O'Brien, W. A review of factors affecting occupant comfort in multi-unit residential buildings. *Build. Environ.* **2019**, *160*, 106182. [\[CrossRef\]](#)
8. Biswas, D.; Szocs, C.; Chacko, R.; Wansink, B. Shining Light on Atmospheric: How Ambient Light Influences Food Choices. *J. Mark. Res.* **2016**, *54*, 111–123. [\[CrossRef\]](#)
9. Atzeri, A.M.; Cappelletti, F.; Tzempelikos, A.; Gasparella, A. Comfort metrics for an integrated evaluation of buildings performance. *Energy Build.* **2016**, *127*, 411–424. [\[CrossRef\]](#)
10. Cerne, B.; Kralj, A.; Drev, M.; Žnidaršič, M.; Hafner, J.; Petter, B. Investigations of 6-pane glazing: Properties and possibilities. *Energy Build.* **2019**, *190*, 61–68. [\[CrossRef\]](#)

11. Ghosh, A.; Norton, B.; Mallick, T.K. Influence of atmospheric clearness on PDLC switchable glazing transmission. *Energy Build.* **2018**, *172*, 257–264. [\[CrossRef\]](#)
12. Ghosh, A.; Norton, B.; Duffy, A. Effect of sky clearness index on transmission of evacuated (vacuum) glazing. *Renew. Energy* **2017**, *105*, 160–166. [\[CrossRef\]](#)
13. Ghosh, A.; Norton, B.; Duffy, A. Effect of sky conditions on light transmission through a suspended particle device switchable glazing. *Sol. Energy Mater. Sol. Cells* **2017**, *160*, 134–140. [\[CrossRef\]](#)
14. Ghosh, A.; Norton, B.; Duffy, A. Effect of atmospheric transmittance on performance of adaptive SPD-vacuum switchable glazing. *Sol. Energy Mater. Sol. Cells* **2017**, *161*, 424–431. [\[CrossRef\]](#)
15. Aburas, M.; Soebarto, V.; Williamson, T.; Liang, R.; Ebendorff-Heidepriem, H.; Wu, Y. Thermochromic smart window technologies for building application: A review. *Appl. Energy* **2019**, *255*, 113522. [\[CrossRef\]](#)
16. Tällberg, R.; Jelle, B.P.; Loonen, R.; Gao, T.; Hamdy, M. Comparison of the energy saving potential of adaptive and controllable smart windows: A state-of-the-art review and simulation studies of thermochromic, photochromic and electrochromic technologies. *Sol. Energy Mater. Sol. Cells* **2019**, *200*, 109828. [\[CrossRef\]](#)
17. Ghosh, A.; Norton, B. Advances in switchable and highly insulating autonomous (self-powered) glazing systems for adaptive low energy buildings. *Renew. Energy* **2018**, *126*, 1003–1031. [\[CrossRef\]](#)
18. Abdelhakim, M.; Lim, Y.W.; Kandar, M.Z. Optimum glazing configurations for visual performance in Algerian classrooms under mediterranean climate. *J. Daylighting* **2019**, *6*, 11–22. [\[CrossRef\]](#)
19. Mesloub, A.; Albaqawy, G.A.; Kandar, M.Z. The optimum performance of Building Integrated Photovoltaic (BIPV) Windows under a semi-arid climate in Algerian Office Buildings. *Sustainability* **2020**, *12*, 1654. [\[CrossRef\]](#)
20. Ghosh, A. Potential of building integrated and attached/applied photovoltaic (BIPV/BAPV) for adaptive less energy-hungry building's skin: A comprehensive Review. *J. Clean. Prod.* **2020**, 123343. [\[CrossRef\]](#)
21. Mesloub, A.; Ghosh, A.; Albaqawy, G.A.; Noaime, E.; Alsolami, B.M. Energy and Daylighting Evaluation of Integrated Semitransparent Photovoltaic Windows with Internal Light Shelves in Open-Office Buildings. *Adv. Civil Eng.* **2020**, *2020*. [\[CrossRef\]](#)
22. Saretta, E.; Caputo, P.; Frontini, F. A review study about energy renovation of building facades with BIPV in urban environment. *Sustain. Cities Soc.* **2019**, *44*, 343–355. [\[CrossRef\]](#)
23. Ghosh, A.; Sundaram, S.; Mallick, T.K. Investigation of thermal and electrical performances of a combined semi-transparent PV-vacuum glazing. *Appl. Energy* **2018**, *228*, 1591–1600. [\[CrossRef\]](#)
24. Ghosh, A.; Sarmah, N.; Sundaram, S.; Mallick, T.K. Numerical studies of thermal comfort for semi-transparent building integrated photovoltaic (BIPV)-vacuum glazing system. *Sol. Energy* **2019**, *190*, 608–616. [\[CrossRef\]](#)
25. Wang, M.; Peng, J.; Li, N.; Yang, H.; Wang, C.; Li, X.; Lu, T. Comparison of energy performance between PV double skin facades and PV insulating glass units. *Appl. Energy* **2017**, *194*, 148–160. [\[CrossRef\]](#)
26. Alrashidi, H.; Ghosh, A.; Issa, W.; Sellami, N.; Mallick, T.K.; Sundaram, S. Thermal performance of semitransparent CdTe BIPV window at temperate climate. *Sol. Energy* **2020**, *195*, 536–543. [\[CrossRef\]](#)
27. Alrashidi, H.; Issa, W.; Sellami, N.; Ghosh, A.; Mallick, T.K.; Sundaram, S. Performance assessment of cadmium telluride-based semi-transparent glazing for power saving in façade buildings. *Energy Build.* **2020**, *215*, 109585. [\[CrossRef\]](#)
28. Chemisana, D.; Moreno, A.; Polo, M.; Aranda, C.; Riverola, A.; Ortega, E.; Lamnatou, C.; Domènech, A.; Blanco, G.; Cot, A. Performance and stability of semitransparent OPVs for building integration: A benchmarking analysis. *Renew. Energy* **2019**, *137*, 177–188. [\[CrossRef\]](#)
29. Selvaraj, P.; Ghosh, A.; Mallick, T.K.; Sundaram, S. Investigation of semi-transparent dye-sensitized solar cells for fenestration integration. *Renew. Energy* **2019**, *141*, 516–525. [\[CrossRef\]](#)
30. Roy, A.; Bhandari, S.; Ghosh, A.; Sundaram, S.; Mallick, T.K. Incorporating Solution-Processed Mesoporous WO₃ as an Interfacial Cathode Buffer Layer for Photovoltaic Applications. *J. Phys. Chem. A* **2020**. [\[CrossRef\]](#)
31. Ma, J.; Guo, D. A data review on certified perovskite solar cells efficiency and I-V metrics: Insights into materials selection and process scaling up. *Sol. Energy* **2020**, *209*, 21–29. [\[CrossRef\]](#)
32. Bhandari, S.; Roy, A.; Ghosh, A.; Mallick, T.K.; Sundaram, S. Perceiving the temperature coefficients of carbon-based perovskite solar cells. *Sustain. Energy Fuels* **2020**, *4*, 6283–6298. [\[CrossRef\]](#)
33. Roy, A.; Ghosh, A.; Bhandari, S.; Sundaram, S.; Mallick, T. Perovskite Solar Cells for BIPV Application: A Review. *Buildings* **2020**, *10*, 129. [\[CrossRef\]](#)
34. Chen, M.; Ju, M.G.; Garcés, H.F.; Carl, A.D.; Ono, L.K.; Hawash, Z.; Zhang, Y.; Shen, T.; Qi, Y.; Grimm, R.L.; et al. Highly stable and efficient all-inorganic lead-free perovskite solar cells with native-oxide passivation. *Nat. Commun.* **2019**, *10*, 16. [\[CrossRef\]](#) [\[PubMed\]](#)
35. Pelle, M.; Lucchi, E.; Maturi, L.; Astigarraga, A.; Causone, F. Coloured BIPV technologies: Methodological and experimental assessment for architecturally sensitive areas. *Energies* **2020**, *13*, 4506. [\[CrossRef\]](#)
36. Røyset, A.; Kolås, T.; Jelle, B.P. Coloured building integrated photovoltaics: Influence on energy efficiency. *Energy Build.* **2020**, *208*. [\[CrossRef\]](#)
37. Ghosh, A.; Sundaram, S.; Mallick, T.K. Colour properties and glazing factors evaluation of multicrystalline based semi-transparent Photovoltaic-vacuum glazing for BIPV application. *Renew. Energy* **2019**, *131*, 730–736. [\[CrossRef\]](#)

38. Roy, A.; Ghosh, A.; Bhandari, S.; Selvaraj, P.; Sundaram, S.; Mallick, T.K. Color Comfort Evaluation of Dye-Sensitized Solar Cell (DSSC) Based Building-Integrated Photovoltaic (BIPV) Glazing after 2 Years of Ambient Exposure. *J. Phys. Chem. C* **2019**, *123*, 23834–23837. [\[CrossRef\]](#)
39. Ahmed, W.; Asif, M. BIM-based techno-economic assessment of energy retrofitting residential buildings in hot humid climate. *Energy Build.* **2020**, *227*, 110406. [\[CrossRef\]](#)
40. Krarti, M.; Howarth, N. Transitioning to high efficiency air conditioning in Saudi Arabia: A benefit cost analysis for residential buildings. *J. Build. Eng.* **2020**, *31*, 101457. [\[CrossRef\]](#)
41. Alardhi, A.; S Alaboody, A.; Almasri, R. Impact of the new Saudi energy conservation code on Saudi Arabia residential buildings. *Aust. J. Mech. Eng.* **2020**, 1–15. [\[CrossRef\]](#)
42. Mesloub, A.; Ghosh, A. Daylighting performance of light shelf photovoltaics (LSPV) for office buildings in hot desert-like regions. *Appl. Sci.* **2020**, *10*, 7959. [\[CrossRef\]](#)
43. Mesloub, A.; Ghosh, A.; Touahmia, M. Performance Analysis of Photovoltaic Integrated Shading Devices (PVSDs) and Semi-Transparent Photovoltaic (STPV) Devices Retrofitted to a Prototype Office Building in a Hot Desert Climate. *Sustainability* **2020**, *12*, 10145. [\[CrossRef\]](#)
44. Imam, A.A.; Al-Turki, Y.A.; Sreerama Kumar, R. Techno-economic feasibility assessment of grid-connected PV systems for residential buildings in Saudi Arabia-A case study. *Sustainability* **2020**, *12*, 262. [\[CrossRef\]](#)
45. Franchini, G.; Brumana, G.; Perdichizzi, A. Monitored performance of the first energy+ autonomous building in Dubai. *Energy Build.* **2019**, *205*, 109545. [\[CrossRef\]](#)
46. Alshawaf, M.; Poudineh, R.; Alhajeri, N.S. Solar PV in Kuwait: The effect of ambient temperature and sandstorms on output variability and uncertainty. *Renew. Sustain. Energy Rev.* **2020**, *134*, 110346. [\[CrossRef\]](#)
47. Ghosh, A.; Bhandari, S.; Sundaram, S.; Mallick, T.K. Carbon counter electrode mesoscopic ambient processed & characterised perovskite for adaptive BIPV fenestration. *Renew. Energy* **2020**, *145*, 2151–2158. [\[CrossRef\]](#)
48. Guo, Y.; Shoyama, K.; Sato, W.; Nakamura, E. Polymer Stabilization of Lead(II) Perovskite Cubic Nanocrystals for Semitransparent Solar Cells. *Adv. Energy Mater.* **2016**, *6*, 1–9. [\[CrossRef\]](#)
49. Chen, W.; Zhang, J.; Xu, G.; Xue, R.; Li, Y.; Zhou, Y.; Hou, J.; Li, Y. A Semitransparent Inorganic Perovskite Film for Overcoming Ultraviolet Light Instability of Organic Solar Cells and Achieving 14.03% Efficiency. *Adv. Mater.* **2018**, *30*, 1800855. [\[CrossRef\]](#) [\[PubMed\]](#)
50. Alrashidi, H.; Ghosh, A.; Issa, W.; Sellami, N.; Mallick, T.K.; Sundaram, S. Evaluation of solar factor using spectral analysis for CdTe photovoltaic glazing. *Mater. Lett.* **2019**, *237*, 332–335. [\[CrossRef\]](#)
51. Ghosh, A.; Selvaraj, P.; Sundaram, S.; Mallick, T.K. The colour rendering index and correlated colour temperature of dye-sensitized solar cell for adaptive glazing application. *Sol. Energy* **2018**, *163*, 537–544. [\[CrossRef\]](#)
52. En, B.S. *Glass in Building—Determination of the Emissivity*; EPB: Chattanooga, TN, USA, 2001.
53. Ghosh, A.; Norton, B. Interior colour rendering of daylight transmitted through a suspended particle device switchable glazing. *Sol. Energy Mater. Sol. Cells* **2017**, *163*, 218–223. [\[CrossRef\]](#)
54. Hernández-Andrés, J.; Lee, R.L.; Romero, J. Calculating correlated color temperatures across the entire gamut of daylight and skylight chromaticities. *Appl. Opt.* **1999**, *38*, 5703–5709. [\[CrossRef\]](#) [\[PubMed\]](#)
55. Nundy, S.; Ghosh, A. Thermal and visual comfort analysis of adaptive vacuum integrated switchable suspended particle device window for temperate climate. *Renew. Energy* **2020**, *156*, 1361–1372. [\[CrossRef\]](#)
56. Ghosh, A.; Mallick, T.K. Evaluation of optical properties and protection factors of a PDLC switchable glazing for low energy building integration. *Sol. Energy Mater. Sol. Cells* **2017**, *176*, 391–396. [\[CrossRef\]](#)
57. Webb, A.R. Considerations for lighting in the built environment: Non-visual effects of light. *Energy Build.* **2006**, *38*, 721–727. [\[CrossRef\]](#)
58. McCamy, C.S. Correlated color temperature as an explicit function of chromaticity coordinates. *Color Res. Appl.* **1992**, *17*, 142–144. [\[CrossRef\]](#)
59. l'Eclairage, C.I. *De CIE 1988 2 Spectral Luminous Efficiency Function for Photopic Vision*; International commission on illumination: Vienna, Austria, 1990; Volume 86.
60. Zhang, F. Evaluation of changing the components involved in CIE color rendering index. *Optik* **2020**, *219*, 165261. [\[CrossRef\]](#)